Journal of Catalysis 274 (2010) 84–98

Contents lists available at ScienceDirect

Journal of Catalysis

journal homepage: www.elsevier.com/locate/jcat

On the selectivity of cobalt-based Fischer–Tropsch catalysts: Evidence for a common precursor for methane and long-chain hydrocarbons

Sara Lögdberg [a], Matteo Lualdi [a], Sven Järås [a], John C. Walmsley [b], Edd A. Blekkan [c], Erling Rytter [c,d], Anders Holmen [c,*]

[a] Royal Institute of Technology (KTH), Chemical Technology, SE-100 44 Stockholm, Sweden
[b] SINTEF Materials and Chemistry, NO-7469 Trondheim, Norway
[c] Norwegian University of Science and Technology (NTNU), Department of Chemical Engineering, NO-7491 Trondheim, Norway
[d] Statoil Technology Centre Trondheim, Arkitekt Ebbells vei 10, NO-7005 Trondheim, Norway

ARTICLE INFO

Article history:
Received 12 March 2010
Revised 21 May 2010
Accepted 14 June 2010
Available online 22 July 2010

Keywords:
Fischer–Tropsch
Cobalt
Selectivity
ASF
Alpha value
Methane
Water
H_2/CO ratio

ABSTRACT

A total of 36 cobalt-based supported catalysts were investigated in the Fischer–Tropsch reaction at industrially relevant process conditions: 483 K, 20 bar, molar H_2/CO ratio = 2.1, pellet size: 53–90 μm. The effect of adding water vapour to the feed was investigated for 20 of the catalysts, and a H_2/CO ratio of 1.0 was used for a few catalysts. The catalysts differed in support material, Co loading, promoters, Cl content, Co particle size (larger than ~6 nm), morphology, degree of reduction and preparation technique and showed a large variation in selectivity. For each set of process conditions, a linear relationship seems to exist between the selectivity to methane (and other light products) and C_{5+} indicating a common precursor, i.e. a common monomer pool, for all hydrocarbon products. A high selectivity to C_{5+} is mainly an effect of a high intrinsic chain-growth probability and unlikely to be a result of an enhanced α-olefin readsorption. The universal effect of external water addition on the hydrocarbon selectivities is limited to a decrease in the methane selectivity. A small proportion of the catalysts developed "pure methanation" sites upon exposure to high partial pressures of water.

1. Introduction

In the Fischer–Tropsch (FT) synthesis, hydrocarbons (HCs) are produced from synthesis gas (H_2 + CO) at elevated pressure, typically over a cobalt- or iron-based catalyst. Due to the FT mechanism of stepwise chain growth, the highest yield to FT diesel is achieved by first making waxes, i.e. very long hydrocarbon chains, and then hydrocracking these into the diesel fraction (~C_{12}–C_{18}). In this way, the production of lighter by-products is minimised. The typical FT-product distribution with respect to carbon number is called the Anderson–Schulz–Flory (ASF) distribution, in which the chain-growth probability (α value) is assumed to be constant and therefore independent of chain length. The ability of a catalyst to produce higher hydrocarbons is often indicated by the α value or by the industrially relevant parameter S_{C5+} (selectivity to C_5 and higher hydrocarbons). Naturally, a higher S_{C5+} results in a more efficient conversion from synthesis gas to diesel fuel.

Provided that the synthesis gas has the correct H_2/CO ratio (approx. 2), supported cobalt catalysts are preferred in the FT process when waxes are the desired product, due to the reasonable price of the metal, high activity and high selectivity to higher hydrocarbons and low water–gas shift activity. For the obtained product distributions over Co-based catalysts, there are always some deviations from the ASF model. For instance, two different α values are often used to describe the product distribution: one lower (α_1) for carbon numbers between ~5 and ~10–20 and one higher (α_∞) for higher carbon numbers [1,2]. Furthermore, the selectivity to methane (S_{C1}) is always significantly higher and that to C_2 (S_{C2}) significantly lower than predicted by the ASF model [3], while for standard alkalised Fe-based catalysts, the C_1 and C_2 fractions are not deviating significantly from an ASF distribution [4–6]. The main products from the Co-catalysed FT synthesis are linear paraffins and olefins. The α-olefins may readsorb on the catalyst and react further to produce longer HCs (reinsertion or initiation) or they may be hydrogenated to form the corresponding paraffins.

Several reasons have been proposed for the higher α value for higher HCs. It could be the result of a higher degree of α-olefin readsorption (due to chain-length-dependent diffusion rate, solubility in wax and/or physisorption) followed by further chain growth [1,2,7,8] or two different chain-growth mechanisms with different monomers on one [9,10] or two [11] type/s of active site/s. The occurrence of different catalytic sites with different chain-growth probabilities [12] and two different termination

* Corresponding author. Fax: +47 73595047.
E-mail address: holmen@chemeng.ntnu.no (A. Holmen).

0021-9517/$ - see front matter © 2010 Elsevier Inc. All rights reserved.
doi:10.1016/j.jcat.2010.06.007

pathways occurring on the same type of site [13] has also been proposed. However, constant α values for the C_{5+} fraction for a number of Co-based catalysts under different process conditions have also been reported [14], as well as a smoother increase in α value with carbon number ascribed to a successive increase in the true propagation probability with carbon number [15]. Some of the observed deviations from ASF have been questioned and attributed to artefacts associated with product analyses [14–16]. The high S_{C1} has been explained by an increased surface mobility of the methane precursor [13] and by different reaction mechanisms and/or active sites for methanation (dissociation of CO) and chain growth (CO insertion) [6,17,18]. The low selectivity to C_2 has been explained by a much higher readsorption rate constant for ethene compared to higher α-olefins [1,14].

The differences in S_{C5+} for Co-based catalysts have been attributed to different extents of α-olefin readsorption (followed by further chain growth) [2], the extent of α-olefin readsorption in turn being governed by the degree of mass transfer restrictions on the product removal (i.e. pore size, catalyst pellet size, active site density and porosity). The importance of secondary reactions on the S_{C5+} has, however, recently been questioned [19–21] and Co particle size effects [20,22,23], as well as effects of the support material [20], on the intrinsic chain-growth probability and, accordingly, on the S_{C5+} have been presented. The observed increase in olefin/paraffin (o/p) ratio, for a certain carbon number, with S_{C5+} was interpreted as if the contribution of α-olefin readsorption to an increased S_{C5+} could only be of minor importance [20]. Recently, it was reported that for Co supported on carbon nanofibres, i.e. a possible inert support material, the S_{C5+} increases with Co particle size up to 6 nm, after which it levels out [23]. This was found to be due to a decreasing surface coverage of hydrogen with increasing Co particle size up to 6 nm. Differences in surface coverages have also been suggested to govern the S_{C5+} for catalysts with Co particles larger than 6 nm [24,25].

Proposed reasons for the well-documented increase in S_{C5+} upon a lowered space velocity (increased conversion) include increased α-olefin readsorption due to the longer bed residence time [1,5] and increased partial pressure of water [21,26,27]. The promoting effect of water on the S_{C5+} has been proposed to be due to its inhibition of hydrogenation reactions, by competitive adsorption, yielding lower methane selectivity and higher probability of olefin readsorption and further growth [18,28,29], as well as due to an increased surface coverage of the active surface carbon (i.e. the monomer pool) [30].

Although relatively mature, there are obviously still uncertainties regarding some fundamental aspects of the Co-catalysed FT synthesis process, in particular the parameters governing the product selectivity of catalysts with Co particles larger than approximately 6 nm on different support materials (under conditions where mass transfer limitations on reactants arrival are absent). In the present paper, selectivity results from careful experimental studies of a range of Co-based catalysts are presented and discussed with focus on evaluating the possible importance of secondary reactions and separate methanation sites on the S_{C5+}. Discussing in detail what characteristics give a catalyst high S_{C5+} is outside the scope of the present paper.

2. Experimental

2.1. Preparation of catalysts

A total of 36 Co-based supported catalysts were prepared. Two different preparation techniques were used: incipient wetness impregnation (IW) and microemulsion (ME). The catalysts were prepared on three different support materials (γ-Al_2O_3, α-Al_2O_3 and TiO_2), with varying Co loadings (4–30 wt%), promoters (Re (0 or 0.5 wt%) or B (0–0.15 wt%)). In addition, two IW-γ-Al_2O_3 catalysts contained residues of Cl, as they were prepared from $CoCl_2$. Furthermore, three catalysts were exposed to hydrothermal treatment (HT) after being prepared by the IW or ME techniques, and one IW-prepared catalyst was additionally reduced and oxidised (RedOx). It should be mentioned that the ME-prepared catalysts contained residues of B from the preparation (0.03 wt% for the ME-α-Al_2O_3 and 0.15–0.18 wt% for ME-γ-Al_2O_3 and ME-TiO_2), while essentially all Cl from the preparation of these ME catalysts was removed in the wash (<0.02 wt% left).

The γ-Al_2O_3 (Puralox SCCa-5/200 from Sasol) and TiO_2 (Degussa P25) support materials were dried at 393 K for 6 h and then calcined in flowing air for 10 h at 773 K and 973 K (ramp = 1 K/min), respectively. The α-Al_2O_3 support was prepared from the γ-Al_2O_3 support by calcining it in flowing air at 1373 K for 10 h. For both the TiO_2 and α-Al_2O_3 support materials, actually three different batches were used that differed slightly in physical properties.

For the IW preparations, the support materials were impregnated with aqueous solutions of $Co(NO_3)_2{\cdot}6H_2O$ (ACS reagent, $\geqslant$99.0%, Fluka) and, in some cases, $HReO_4$ (Alfa Aesar) or B_2O_3 ($\geqslant$98.0%, Fluka). In two cases, an aqueous solution of $CoCl_2{\cdot}6H_2O$ (99.9% (metals basis), Alfa Aesar) was used instead of cobalt nitrate. Three impregnations, with intermediate drying at 373 K for 1 h, were used. The powder was then dried at 393 K for 3 h and calcined in air at 573 K for 16 h (ramp = 1 K/min) in a crucible standing in the oven. One of the IW catalysts prepared from $CoCl_2$ was, however, calcined at 773 K as $CoCl_2$ was found not to decompose at the lower temperature. The Cl contents of the IW catalysts prepared from $CoCl_2$, prior to reduction, were 7.7 wt% (calcined at 573 K) and 1.5 wt% (calcined at 773 K), respectively.

For the ME preparations, the following components were mixed in order to form the microemulsion:

Oil phase (69.8 wt%): cyclohexane (ACS reagent, $\geqslant$99.0%, Sigma Aldrich)
Surfactant (19.9 wt%): Berol 02, polyoxyethylene (6) nonylphenyl ether (Akzo Nobel)
Water phase (10.3 wt%): aqueous solution of $CoCl_2{\cdot}6H_2O$ (99.9% (metals basis), Alfa Aesar) and $HReO_4$ (Alfa Aesar). $[Co^{2+}]$ in water phase: 0.12 M. $[Re^{7+}]$ in water phase: 1.6 mM.

In order to form a sol (i.e. solid Co-containing particles dispersed in the oil phase) from the microemulsion, a $NaBH_4$ (98% min, Alfa Aesar) aqueous solution (10 M) was added as a reducing agent. A molar ratio of BH_4^-/Co^{2+} of 3 was used. The reduction step was performed in a N_2 atmosphere in a glove bag. The Co-containing particles were deposited onto the supports by destabilisation of the organosol with acetone (50 cm^3 acetone/100 g sol) in the presence of the support under vigorous stirring for 2–3 h. In total, for γ-Al_2O_3 and TiO_2, six depositions were made in which approximately 2 wt% of Co (and 0.083 (=0.5/6) wt% Re) was added to the support in each deposition to finally reach a Co loading of 12 wt%. For α-Al_2O_3, a Co loading not higher than 4.4 wt% was achieved after 10 depositions, as only a small proportion of the Co particles were attached to the support. After each deposition, the catalyst powders were washed with ethanol, acetone and water at room temperature and then dried at 323 K overnight. After the last deposition, the water for the wash had a temperature of 373 K. After the final deposition and wash, the ME catalysts were dried for at least 16 h at 323 K and then calcined in air at 573 K for 16 h (ramp = 1 K/min). The majority of the added Re was found to be removed in the wash.

In the hydrothermal treatment mentioned above, three catalysts were exposed to water vapour at 873 K in flowing air for 5 h. The one catalyst exposed to the RedOx treatment mentioned above was, after being prepared according to the IW procedure,

first reduced in hydrogen at 623 K for 16 h, then passivated (in N_2 5.0 for 0.5 h and in 0.5 vol% O_2 in N_2 for 1 h at room temperature) and finally calcined again in air at 573 K for 16 h.

2.2. Catalyst characterisation techniques

Brunauer–Emmett–Teller (BET) surface area and porosity measurements for the γ-Al_2O_3-supported catalysts were performed in a Micromeritics ASAP 2000/2010 unit. The samples were evacuated and dried at 523 K overnight prior to analysis. The BET area was estimated by N_2 adsorption at liquid nitrogen temperature at relative pressures between 0.06 and 0.2. The total pore volume was estimated from a single point of adsorption at $p/p^0 = 0.998$, and the average pore diameter was estimated from the pore volume and BET surface area assuming cylindrical pores. Internal surface area and porosity measurements for the α-Al_2O_3 and TiO_2-supported catalysts were performed in a Micromeritics Mercury Porosimeter, AutoPore IV.

Oxygen titration was performed in order to estimate the degree of reduction (*DOR*) of the catalysts after reduction under flowing hydrogen for 16 h at the reduction temperature used prior to FT experiments (623 or 673 K) and has been described elsewhere [31,32]. The *DOR* was calculated assuming that all cobalt in metallic form was oxidised to Co_3O_4.

The *DOR* was also estimated from temperature programmed reduction (TPR) of the reduced samples: after reduction in flowing hydrogen for 16 h at 623/673 K, the samples were purged with helium for 1 h at the reduction temperature, then brought down to room temperature in flowing helium and finally TPR was performed. The catalyst samples were heated at a rate of 10 K/min to 1203 K in a flow of 7% H_2 in argon. The hydrogen consumption was measured by comparing the thermal conductivity of the inlet and outlet gas. Calibration was done by the reduction of Ag_2O powder. The *DOR* was calculated assuming that the unreduced cobalt in the reduced catalysts (after 16 h at 623/673 K) was composed of Co(II) as evidenced from X-ray absorption spectroscopy [33].

The procedure of measuring H_2 adsorption isotherms of the catalysts, in order to estimate the Co dispersion (*D*, %), has been described elsewhere [31,32]. Briefly, the measurements were conducted on a Micromeritics ASAP 2010 unit at 313 K, after reducing the calcined catalysts in flowing hydrogen at 623/673 K for 16 h. Since the chemical adsorption of H_2 on Co has been reported to be reversible [34] and since physical adsorption of H_2 on Co is negligible [35], the adsorption data from a single isotherm were used for dispersion estimates. It was assumed that the adsorption stoichiometry is 1 H_2 on 2 Co (or H:Co = 1) [36] and that Re does not contribute to the amount of hydrogen adsorbed. The particle size (*d*, nm) of Co^0 is estimated according to the following equation [20,37]:

$$d = \frac{96}{D} \cdot DOR \tag{1}$$

Reduced (in hydrogen at 623/673 K for 16 h) and passivated (in N_2 5.0 for 0.5 h and in 0.5 vol% O_2 in N_2 for 1 h at room temperature) catalysts were prepared for transmission electron microscopy (TEM) by ultramicrotomy after first embedding in an organic resin. TEM analysis was performed using a JEOL 2010F instrument operating at 200 kV equipped with an Oxford Instruments X-ray detector for energy dispersive spectroscopy (EDS) composition analysis. Conventional TEM was performed under bright-field diffraction contrast conditions. For EDS, the microscope was operated in scanning transmission electron microscopy (STEM) mode with a nominal probe diameter of ~0.7 nm. STEM images were acquired using an annular dark field detector, which provides contrast that has a strong dependence on atomic number.

X-ray diffraction (XRD) was performed on the calcined and/or reduced and passivated samples using a Siemens D5005 X-ray diffractometer with Cu Kα radiation. A secondary monochromator was used. Crystallite thicknesses of Co_3O_4 and/or Co were estimated by using the Scherrer formula [35]. Assuming spherical crystallites, the diameter of the particles was estimated by correcting the crystallite thickness by a factor 4/3 [35]. When the Co crystallite size was estimated from that of Co_3O_4, the following formula was used [38]:

$$d(Co^0) = 0.75 \cdot d(Co_3O_4) \tag{2}$$

according to the relative molar volumes of metallic cobalt and Co_3O_4.

2.3. Fischer–Tropsch experiments

A detailed description of the equipment and procedure has been given elsewhere [19,32]. Briefly, FT synthesis was performed in a stainless-steel fixed-bed reactor (i.d. 10 mm) at the following reference case process conditions: 483 K, 20 bar, molar H_2/CO ratio = 2.1, catalyst pellet size: 53–90 μm. The catalysts were diluted with SiC to achieve an even temperature profile and reduced *in situ* in hydrogen for 16 h at atmospheric pressure prior to the FT experiments, at 623 K and 673 K for IW and ME-prepared catalysts, respectively, as the ME catalysts had significantly lower reducibilities. Also, the two Cl-containing IW catalysts were reduced at 673 K.

Initial reactant flow (period A) was 250 N cm^3/min (or gas hourly space velocity 5000–15,000 N cm^3/g_{cat}, h depending on amount of catalyst) and held for approximately 24 h. Then, the space velocity was lowered to achieve approximately 40% CO conversion (period B) and held for another 24 h. A total of 20 of the catalysts were held further on stream and exposed to different amounts of water vapour in the feed the following 48 h (20% in period C and 33% in period D). Water vapour was introduced by passing deionised water through an electrical vaporiser kept at 623 K and mixed with the synthesis gas prior to the reactor inlet. The total pressure and flow of synthesis gas were kept constant during external water addition, which implies that the partial pressures of the reactants were lower in periods C and D. In the last period (E) for these 20 catalysts, the water feed was shut off, and the experimental conditions were the same as in period B. The different periods (A–E) are illustrated in Figs. 1 and 2. A small proportion of the catalysts were also tested under a molar H_2/CO ratio of 1.0.

The heavy HCs and most of the liquid products were collected in a heated trap (363 K). The product gases also passed through a "cold" trap at room temperature in order to condense residual liquid products, before gas analysis. The product gases (C_1–C_6 HCs and CO_2), as well as N_2 and unconverted CO, were analysed on line by a HP 5890 gas chromatograph equipped with a thermal conductivity detector (TCD) and a flame ionisation detector (FID). N_2 was used as an internal standard. Quantitative analyses of C_1–C_4 HCs were performed and allowed for S_{C5+} determination. The S_{C5+} is defined as follows (after correction for the low S_{CO_2} (<2% in dry periods)):

$$S_{C5+} = 100 - (S_{C1} + S_{C2} + S_{C3} + S_{C4}) \tag{3}$$

Quantitative analyses of C_5 and C_6 HCs existing in the gas phase were also made. By assuming gas/liquid equilibrium in the cold trap (calculated by using Aspen HYSYS 2006, equation of state: Lee Kesler Plocker, 298 K, 20 bar), the total amount of C_5 and C_6 HCs could be estimated from the gas analysis. Formation of oxygenates over these Co-based catalysts has been assumed negligible. All reported selectivities are C-atom based and CO_2-free.

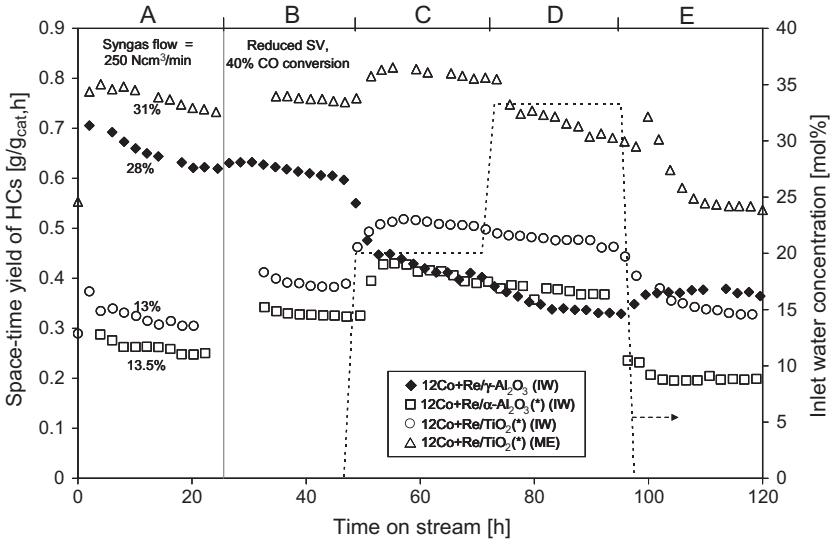

Fig. 1. Space-time yields of hydrocarbons for three IW catalysts (12 wt% Co, 0.5 wt% Re) and the ME-TiO_2 catalyst during 5 days on stream. The %-numbers in the first period indicate the CO conversions in the middle of period A. After 24 h on stream, the space velocity (SV) (and accordingly the synthesis gas flow) was lowered so as to reach a CO conversion of 40% (period B). The same synthesis gas flow was used during periods C, D and E. Water vapour was added to the feed, in different amounts, during the third and fourth day (C and D). Reaction conditions: 483 K, P_{tot} = 20 bar, H_2/CO = 2.1 (the synthesis gas pressure was reduced upon water introduction since no correction with inert gas was made).

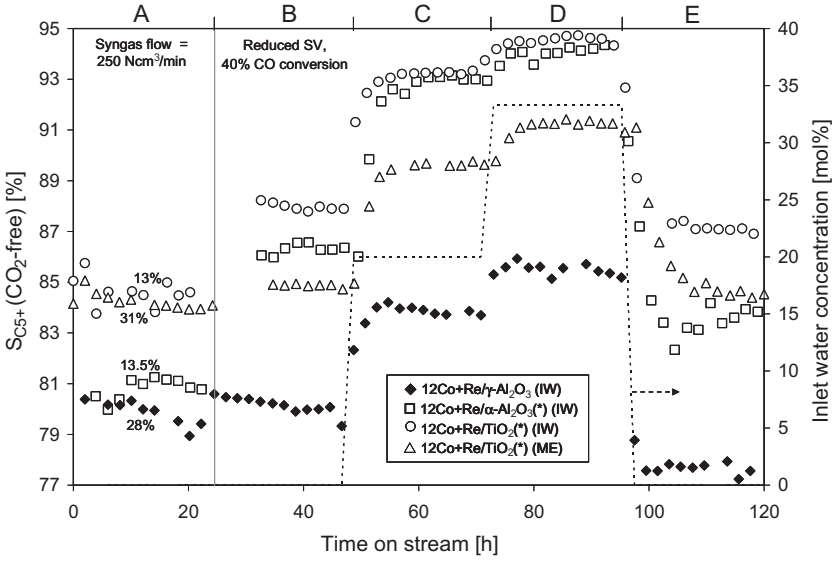

Fig. 2. S_{C5+} vs. time on stream for the catalysts shown in Fig. 1.

3. Results

3.1. Characterisation of catalysts

Table 1 shows the physical properties of the pure support materials and of some selected catalysts. The γ-Al_2O_3 is a typical narrow-pore support with high surface area, while α-Al_2O_3 and TiO_2 have larger pores and lower surface areas. The α-Al_2O_3 was prepared by heat treatment of the γ-Al_2O_3, as mentioned in Section 2.1.

Table 2 shows the physicochemical properties of all studied catalysts. The number in front of the element (Co or B) indicates the loading in wt%. For all Re-promoted catalysts, the nominal loading was 0.5 wt% Re but, as mentioned in Section 2.1, the Re content in the ME catalysts was significantly lower. The *DOR* (degree of reduction) of the catalysts, as measured by oxygen titration, varied between 22% and 71%. The *DOR* estimated from TPR measurements were significantly higher and, probably, more correct as reported earlier [19]. Hence, this *DOR* was used together with dispersion measurements for cobalt particle size estimations (according to Eq. (1) above), which ranged between 6 and 42 nm. All catalysts, except for the ME-γ-Al_2O_3 catalyst, had crystalline Co particles, as evidenced from XRD.

When using the IW technique, the large-pore supports (α-Al_2O_3 and TiO_2) resulted in larger Co particles than the narrow-pore γ-Al_2O_3, which is a well-known phenomenon [19,32,39]. When using the ME technique with α-Al_2O_3 and TiO_2, the resulting Co particle sizes were similar to that of the IW-γ-Al_2O_3 catalysts (prepared from $Co(NO_3)_2$) and approximately half of the size in the corresponding IW catalysts (for the same batch of support material). Increasing the Co loading in the IW preparations generally increased both the Co_3O_4 crystallite size in the calcined catalysts

Table 1
Physical properties of the pure support materials and of some selected catalysts. IW, incipient wetness impregnation; ME, microemulsion.

Catalyst	Average pore diameter[a] (nm)	Surface area (A) (m^2/g_{cat})	Pore volume (V) (cm^3/g_{cat})
γ-Al_2O_3	10.4	193	0.5
6Co (IW)	9.6	181	0.44
12Co (IW)	9.3	173	0.40
12Co + Re (IW)	8.9	172	0.38
20Co (IW)	8.5	148	0.31
12Co + Re (ME)	10.2	201	0.51
α-Al_2O_3	72	11.7	0.21
6Co (IW)	66	10.4	0.17
12Co (IW)	62	10.4	0.16
20Co (IW)	50	10.4	0.13
α-$Al_2O_3(*)$	65	11.1	0.18
12Co + Re (IW)	58	8.3	0.12
4.4Co + Re (ME)	57	11.3	0.16
TiO_2	193	26.1	1.26
6Co (IW)	106	17.4	0.46
12Co (IW)	90	15.5	0.35
20Co (IW)	111	13.7	0.38
30Co (IW)	91	12.7	0.29
$TiO_2(*)$	257	23.2	1.49
12Co + Re (IW)	273	13.2	0.90
12Co + Re (ME)	174	20.2	0.88

[a] The average pore diameter (d_p) estimated from surface area (A) and pore volume (V) according to: $d_p = \frac{4V}{A}$.

and the Co particle size in the reduced catalysts. The Co loading, as well as Re promotion, had a strong influence on the *DOR* of γ-Al_2O_3-supported catalysts, while a much less pronounced effect was found for the other catalysts. This may be ascribed to Co(II) ions entering some of the tetrahedral vacancies of the defect spinel structure of γ-Al_2O_3 upon reduction [40]. Re inhibits the formation of these hard-to-reduce Co-support species and also facilitates the reduction of CoO interacting strongly with γ-Al_2O_3 [41]. As seen from Table 2, there was no unequivocal effect on the Co particle size of the addition of 0.5 wt% Re to the 12 wt% Co catalysts. The addition of 0.15 wt% B, however, seemingly reduced the Co_3O_4 crystallite size, as reported earlier [42], while the effect on the Co particle size is unclear. Addition of B clearly decreased the *DOR* [42].

The dispersion measurements on the two Cl-containing IW catalysts largely overestimated the Co particle sizes, probably due to residual Cl being adsorbed onto the Co sites. Hence, XRD of the reduced and passivated samples was used for particle size estimation instead. By using $CoCl_2$ instead of the nitrate, significantly larger Co particles were formed on γ-Al_2O_3; 25 and 16 nm for the $CoCl_2$-based catalysts calcined at 573 K and 773 K, respectively, compared to 9 nm for the corresponding $Co(NO_3)_2$-based catalyst calcined at 573 K (as measured from XRD of reduced and passivated samples, see Table 2). The morphologies of the Cl-containing IW catalysts were also found to be very different. Fig. 3a illustrates the Co distribution in the IW-γ-Al_2O_3 catalyst prepared from $Co(NO_3)_2$ where Co particles form aggregates within the support pore structure [43]. Fig. 3b illustrates the Co distribution in the IW-γ-Al_2O_3 catalyst prepared from $CoCl_2$, in which no Co particle aggregates were found. Of course, not only the choice of Co precursor but also the choice of support material greatly affects the structure of the final catalyst. For example, similar well-defined aggregates of Co particles as illustrated in Fig. 3a were not found in the α-Al_2O_3 or TiO_2-supported catalysts, as seen from Fig. 3c and d, respectively.

The ME technique also yielded a different distribution of the Co particles over the γ-Al_2O_3 and α-Al_2O_3 supports compared to the IW technique. The strongest effect was seen for the γ-Al_2O_3-supported catalyst. Fig. 3e shows that for the ME sample, the small pores of the γ-Al_2O_3 resulted in deposition of a significant proportion of the Co particles on the external surface of the γ-Al_2O_3 pellets, suggesting that the Co particles surrounded by surfactant molecules were generally too big to enter the pores of the γ-Al_2O_3 during destabilisation of the sol. This distribution was confirmed by EDS X-ray analysis and mapping, where a strong Co signal was obtained from the irregular material indicated by arrows, while a comparatively weak Co signal was obtained from within the pellets. As mentioned above, the Co phase of the fresh ME-γ-Al_2O_3 catalyst was XRD amorphous.

The hydrothermal treatment, which was performed with three of the catalysts, increased the Co particle size of the ME-α-Al_2O_3 catalyst (from 11 to 17 nm, estimated from XRD of calcined catalysts), while the Co particle sizes appeared rather unchanged for the IW-γ-Al_2O_3 and IW-α-Al_2O_3 catalysts, as seen in Table 2. The IW-γ-Al_2O_3 catalyst, however, lost a significant part of its FT activity and selectivity to higher HCs, probably due to the formation of inactive Co–Al species during the hydrothermal treatment, as indicated from XRD measurements and from a lowered degree of reduction.

Assuming an unchanged site activity, the RedOx treatment of the IW-TiO_2 catalyst reduced the Co particle size with 25%.

3.2. Activity results

It has been shown that for catalysts with Co particle sizes above approximately 6 nm, the site activity, or turnover frequency (TOF), is relatively constant at constant process conditions [22,23,28,32,44,45] and hence independent of support material and HC selectivities. This is also the case for the majority of the catalysts in the present study (see Table 2), for which the site activity (mol CO converted/mol surface Co, s) after 10 h on stream under reference case process conditions varied mainly between 0.044 and 0.08 s^{-1}. Some of the TiO_2-supported catalysts had higher site activities, but this is probably due to an underestimation of the dispersion due to TiO_x decoration [36].

In Fig. 1, the space-time yields to hydrocarbons vs. time on stream are shown for four selected catalysts with the same nominal loadings (12 wt% Co, 0.5 wt% Re). The higher productivity of the ME-$TiO_2(*)$ catalyst, when compared to its IW counterpart, is a result of the smaller Co particles obtained when using the ME technique. The large-pore-supported catalysts tended to react positively to the external water addition, while the γ-Al_2O_3-supported catalysts generally lowered their FT rates.

3.3. Selectivity results

In Fig. 2, the S_{C5+} vs. time on stream are shown for the same catalysts as shown in Fig. 1. In the following subparagraphs, the selectivities under the reference case process conditions (i.e. periods A and B), as well as under changed conditions (e.g. periods C and D), will be discussed. Also, the effect of time on stream (i.e. periods A and B compared with period E) will be touched upon.

3.3.1. Estimation of α_{Cn} values

The weight fraction W_n of a hydrocarbon chain with n carbon atoms is defined by the ASF model as follows [46,47], assuming that each C-unit has the same weight:

$$W_n = n \cdot (1-\alpha)^2 \cdot \alpha^{n-1} \quad (4)$$

where the propagation probability α is independent of chain length. As a single α value cannot explain the true product selectivity (the deviation is especially large in the C_1–C_5 range), separate α_{Cn} values

Table 2
Physicochemical properties, TOF in period A (after 10 h on stream) and S_{C5+} in period B of the studied catalysts. IW: incipient wetness impregnation. ME: microemulsion. HT: hydrothermally treated.

Catalyst	Reduction temperature (K)	*DOR*, O_2 titr. (%)	*DOR*, TPR (%)	*DOR* used in calculations[a] (%)	Co dispersion (%)	Co particle size (from *DOR* + disp.)[b] (nm)	Co_3O_4 cryst. size in calcined catalyst (XRD) (nm)	Co cryst. size (XRD)[c] (nm)	TOF after 10 h on stream[d] (s^{-1})	S_{C5+} in period B (%)
γ-Al_2O_3										
6Co (IW)	623	52	50	50	7.6	6	13	10	0.059	79.3
8Co (IW)	623	46	–	54	7.1	7	13	10	0.050	79.1
12Co (IW)	623	51	62	62	7.5	8	15	11	0.044	79.0
12Co + Re (IW)	623	63	92	92	9.7	9	16	12 [9]	0.066	80.3
12Co + Re (IW) HT	623	37	–	–	–	–	16	12	–	75.0
20Co (IW)	623	–	65	65	7.1	9	16	12	0.065	79.1
12Co + Re (ME)	673	22	67	67	5.0	13	amorph.	[amorph.]	0.026	69.1
12Co + 0.15B (IW)	623	48	56	56	7.4	7	14	11	0.059	82.1
12Co + Re (IW) CI 573 K[e]	673	58	–	–	0.4	–	$CoCl_2$	[25]	–	55.5
12Co + Re (IW) CI 773 K	673	37	–	–	0.9	–	18	[16]	–	69.0
α-Al_2O_3										
4Co (IW)	623	–	98	98	7.5	13	29	22	0.044	85.7
6Co (IW)	623	–	–	98	5.2	18	34	26	0.044	84.8
12Co(IW)	623	–	99	99	4.3	22	26	20	0.049	84.0
12Co + Re(IW)	623	–	–	99	4.5	21	25	19	0.058	84.9
20Co (IW)	623	–	99	99	2.3	42	45	34	0.045	81.6
α-Al_2O_3(∗)										
12Co + Re (IW)	623	67	–	99	3.5	27	44	33	0.071	86.5
12Co + Re (IW) HT	623	62	–	92	3.4	26	47	35	0.059	84.0
4.4Co + Re (ME)	673	61	–	90	7.3	12	14	11	0.050	77.4
4.4Co + Re (ME) HT	673	60	–	89	3.9	22	23	17	0.037	72.6
α-Al_2O_3(∗∗)										
6Co (IW)	623	68	–	98	3.6	26	36	27	0.048	83.3
12Co (IW)	623	68	–	99	4.3	22	33	25	0.047	83.1
TiO_2										
4Co (IW)	623	–	–	92	4.2	21	19	14	0.081	84.1
6Co (IW)	623	–	94	94	4.3	21	21	16	0.070	84.0
12Co (IW)	623	–	96	96	3.9	24	23	17	0.070	84.9
12Co + Re (IW)	623	–	96	96	4.7	20	19	14	0.092	87.2
12Co + Re (IW), RedOx	623	–	–	96	6.2[f]	15	–	–	0.092	89.5
20Co (IW)	623	–	97	97	3.3	28	26	20	0.060	87.1
20Co (IW), less water	623	–	–	97	2.9	32	32	24	0.071	87.7
30Co (IW)	623	–	–	97	2.2	42	37	28	0.054	87.9
12Co + 0.044B (IW)	623	–	92	92	4.4	20	24	18	0.063	84.9
12Co + 0.15B (IW)	623	–	87	87	3.7	22	19	14	0.082	87.0
TiO_2(∗)										
6Co (IW)	623	60	–	94	3.3	28	19	14	0.107	86.0
12Co + Re (IW)	623	70	–	96	3.0	31	29	22	0.104	88.0
12Co + Re (ME)	673	64	89	89	5.5	16	13	10	0.136	84.9
TiO_2(∗∗)										
12Co (IW)	623	71	–	96	4.0	23	24	18	0.074	84.2
12Co + 0.15B (IW)	623	61	–	87	2.9	29	21	16	0.068	89.5

[a] *DOR* from TPR of reduced catalysts where data available. Otherwise estimated from inter-/extrapolations of available *DOR* (from TPR) data, or by comparison of *DOR* (from O_2 titr.) data and "translation" to *DOR* (from TPR).
[b] According to Eq. (1).
[c] Estimated from XRD of calcined samples according to Eq. (2). Bracketed values indicate XRD of reduced and passivated samples.
[d] Turnover frequencies (TOFs) calculated from gas flow rates and CO conversions in period A and from Co dispersion data.
[e] This catalyst was composed of $CoCl_2$ in its calcined state, which was accounted for when calculating *DOR* and Co dispersion.
[f] Calculated by assuming the same TOF as the corresponding catalyst without RedOx treatment.

for $n = 1$–6 (α_{C1}–α_{C6}) have been calculated in the present paper, each indicating the probability of chain growth of the C_n^* surface species. In order to calculate these individual α_{Cn} values, the same approach as described by Bertole et al. [48] has been used. The expressions utilised are as follows [2]:

$$\alpha_{Cn} = \frac{r_{g,n}}{r_{g,n} + r_{t,n}} = \frac{\sum_{m=n+1}^{\infty} r_{Cm}}{\sum_{m=n+1}^{\infty} r_{Cm} + r_{Cn}} \quad (5)$$

where r indicate molar rates, and subscripts g and t growth and termination, respectively. Since only a fraction of the total HC product was quantified (C_1–C_6), it is necessary to make an assumption about the carbon-number distribution of the C_{7+} fraction in order to estimate the molar rates for the same fraction. The C_{7+} fraction is assumed to follow an ASF distribution with the α value that would give the same S_{C7+} as the catalyst in question.

3.3.2. Results at reference case process conditions

The S_{C5+} values in period B for all studied catalysts are given in Table 2. It can be seen that, in general, TiO_2-supported catalysts have the highest S_{C5+}, and γ-Al_2O_3-supported catalysts the lowest. The ME-TiO_2(∗) catalyst has a similar Co particle size as IW-γ-Al_2O_3 (12 wt% Co, 0.5 wt% Re) but a significantly higher S_{C5+}, indicating that a possible Co particle size effect (above 6 nm) is subordinate to the effect of support material. Studying the TiO_2-supported IW catalysts more closely suggests that the S_{C5+} is increasing with Co particle size, while the opposite is true for the α-Al_2O_3-supported IW catalysts. That TiO_x decoration of Co particles reduces the S_{C5+}

has been reported previously [28,49], and the TiO_x decoration should reasonably be more severe the smaller the Co particles

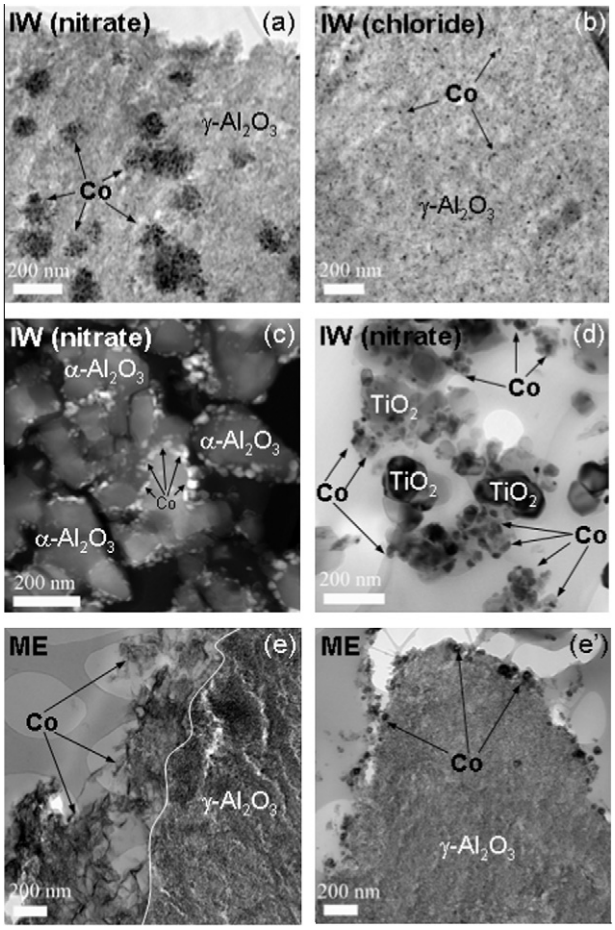

Fig. 3. TEM images of cross-sections of fresh IW-γ-Al_2O_3 (12 wt% Co, 0.5 wt% Re) catalysts prepared from Co nitrate (a) and Co chloride (b), fresh IW-α-Al_2O_3 (12 wt% Co, 0.5 wt% Re) (STEM) (c), fresh IW-TiO_2 (12 wt% Co, 0.5 wt% Re) (d), fresh ME-γ-Al_2O_3 (~12 wt% Co) (e), and used ME-γ-Al_2O_3 (e′). The white line in (e) indicates the γ-Al_2O_3 pellet boundary. The IW-catalyst prepared from $CoCl_2$ (b) was calcined at 773 K.

[50]. Also, a negative correlation between Co particle size and S_{C5+} for α-Al_2O_3-supported catalysts has been shown [20]. The RedOx treatment of IW-TiO_2 (12 wt% Co, 0.5 wt% Re) improves the S_{C5+} significantly, although the Co particle size is apparently reduced. Possibly, the break-up of Co or Co_3O_4 crystallites into smaller particles is connected with this increase in S_{C5+}, which has been suggested earlier [19] for γ-Al_2O_3-supported catalysts. In fact, this "break-up" theory could also explain why smaller Co particles give higher S_{C5+} for α-Al_2O_3-supported IW catalysts, the catalyst with smaller Co particles having the largest $d(Co_3O_4)/dCo^0$ ratio as estimated from XRD of calcined catalyst and from dispersion and *DOR* measurements of reduced catalyst. As already well known, both Re and B enhance S_{C5+} [32,42]. The exceptional increase in S_{C5+} when adding 0.15 wt% B to the IW-TiO_2(**) (12 wt% Co) can be ascribed to the simultaneous increase in Co particle size as estimated from dispersion and *DOR* measurements.

The catalysts presented in Table 2 provide selectivity data over a large range (S_{C5+} in period B: 55.5–89.5%). It is therefore the primary focus of the present paper to discuss possible correlations between the selectivities and, in particular, to investigate the possible importance of secondary reactions and separate methanation sites on the S_{C5+}. Fig. 4 shows the resulting individual α_{Cn} values for $n = 1$–4 vs. S_{C5+}, and Fig. 5 shows the selectivities of C_1–C_4 vs. S_{C5+}, for the catalysts in periods A and B. Note that α_{C1}, defined by Eq. (5) above, has a different meaning from α_1 described in the introduction. Regression lines, calculated by using the method of least squares, are based on data obtained in period B. The goodness of fit for each regression line is represented by the indicated R^2 value. It is striking how well the α_{Cn} values, as well as the selectivities, fit to linear correlations irrespective of support material, Co loading, addition of promoters, preparation technique, Co particle size, degree of reduction and presence of a catalyst poison (Cl). Furthermore, the conversion level does not seem to affect the interdependencies appreciably.

The lower R^2 values of the regression lines of α_{C2} and S_{C2} are partly explained by a higher relative standard deviation of the S_{C2} (~6%) when compared to the S_{C1} (~4%) and the S_{C3} and S_{C4} (~2% each), as estimated from multiple runs with the same catalyst. This is in turn explained by the very low concentration of C_2 products in the effluent gas. Also, the small variation in α_{C2} values around the population average, i.e. the small slope of this regression line, contributes to the lower R^2 value. The higher relative

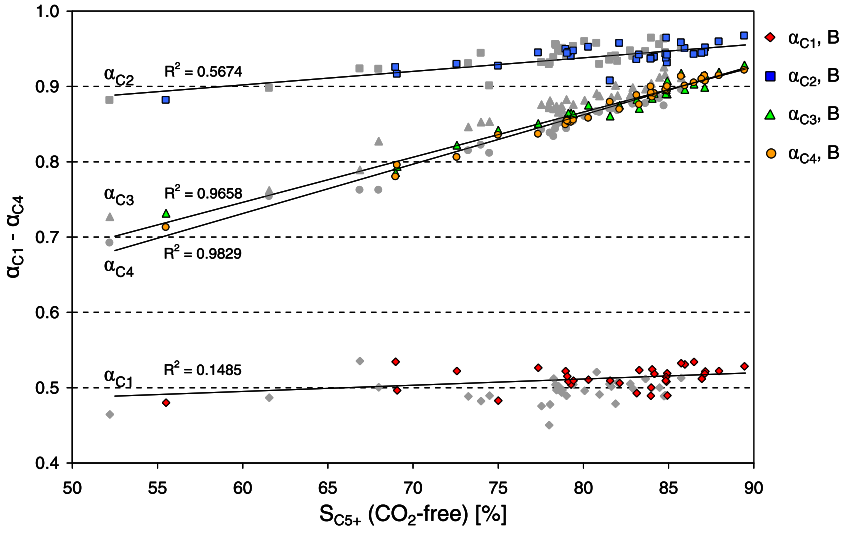

Fig. 4. α_{Cn} values ($n = 1$–4) vs. S_{C5+} for all catalysts in period A (grey symbols) and B (coloured symbols). CO conversion in period A is different for each catalyst varying between 3.5% and 30%. CO conversion in period B is ~40%. Experimental conditions: 483 K, 20 bar, $H_2/CO = 2.1$, pellet size 53–90 μm. Regression lines are based on data points obtained in period B.

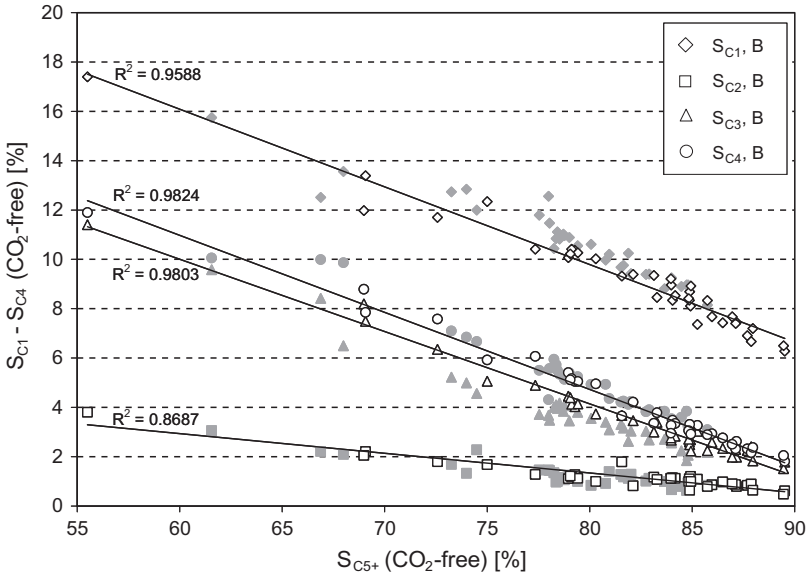

Fig. 5. S_{C1}–S_{C4} vs. S_{C5+} for all catalysts in period A (grey, filled symbols) and B (open symbols). Experimental conditions as in Fig. 4. Regression lines are based on data points obtained in period B.

standard deviation for S_{C1} when compared to those of S_{C3} and S_{C4} probably stems from that S_{C1} is more sensitive to small changes in certain process parameters (e.g. temperature, H_2/CO ratio, partial pressure of water), which is discussed in Section 3.3.4. The α_{C1} has the narrowest range of values (0.48–0.53 in period B) of all estimated α_{Cn} values and, apparently, this small variation in the α_{C1} data points is not well correlated with the S_{C5+} as seen from the very low R^2 value of this regression line (see Fig. 4).

It might be argued that the observed trends shown in Fig. 5 are partly a result of mathematics as the S_{C5+} is a function of the sum of the lower selectivities (see Eq. (3)). However, also S_{C5} and S_{C6} are linearly correlated with S_{C5+} (not shown), despite their higher relative standard deviations (S_{C5}: ~3%, S_{C6}: ~4%) and their mathematical independence of S_{C5+}, which confirms that individual HC selectivities are indeed well correlated with S_{C5+} (at least for the low carbon numbers investigated here). α_{C5} and α_{C6} were found to be nearly identical with α_{C4}, which in turn is very close to α_{C3}, as evidenced from Fig. 4.

One of the catalysts with the poorest S_{C5+} (61.6% in period A and 69.1% in period B, see Table 2) is the amorphous (with respect to cobalt) ME-γ-Al_2O_3, which is not surprising as Co particles smaller than approximately 6–8 nm are known to give low S_{C5+} [20,22,23]. What is interesting is that this catalyst, despite the obvious differences between this and the other catalysts (i.e. non-crystallinity, Co particles located mainly on external surface of support pellet), still falls relatively well on the experimental curves of Figs. 4 and 5. The much shorter diffusion distance for the ME-γ-Al_2O_3 catalyst, compared to the other catalysts that have the Co particles inside the pores of their 53–90 μm pellets, should imply a much lower probability of α-olefin readsorption. This fact, apparently, does not result in a deviation from the trends shown in Figs. 4 and 5.

The catalyst with the absolutely poorest S_{C5+} (52.2% in period A and 55.5% in period B, see Table 2) is the IW-γ-Al_2O_3 catalyst (12 wt% Co, 0.5 wt% Re) prepared from $CoCl_2$ and calcined at 573 K, which is not surprising either as Cl is a known poison to Co-based FT catalysts [51]. The difference in Co particle size when compared to the corresponding catalyst prepared from $Co(NO_3)_2$ (see Table 2) could of course also affect the selectivity, as could the different morphologies. The important issue in the current study is that the selectivities of a catalyst clearly under the influence of a poison follow the same trends as observed for non-poisoned catalysts. Furthermore, different morphologies of the catalysts, apparently, do not affect the interdependencies between the selectivities/α_{Cn} values.

Puskas et al. [14] reported that the C_2–C_4 products obtained over supported Co catalysts were nearly constant fractions of the values expected from the corresponding ASF distributions (calculated from the α value based on the C_6–C_{10} products), depending little on the experimental conditions. This is essentially in agreement with the observations in the present study, with the difference that we have also found that there is a correlation between the C_1 product and the estimated α_{Cn} values (i.e. α_{C2}–α_{C6}) at fixed process conditions. Also, Mims and Bertole [24] have reported on a correlation between S_{C1} and a "α value" estimated from the S_{C5+}/S_{C4} ratio, and Iglesia et al. [52] found a constant termination probability of C_1^* (and hence a constant α_{C1}) for a range of different Co catalysts at conditions similar to the reference case process conditions in the present paper. However, these studies were based on relatively narrow ranges of S_{C5+} values.

3.3.3. Olefin/paraffin ratios

A reduced space velocity (i.e. increased *bed* residence time) increases the extent of readsorption mainly of short α-olefins [1], and the accompanying increase in S_{C5+} has been attributed to this readsorption (followed by chain growth) [2]. In Fig. 6, the percentage increase in S_{C5+} vs. the percentage decrease in C_3 o/p (olefin/paraffin) ratio upon a halving of the space velocity has been plotted for all catalysts. The high values of the ME-γ-Al_2O_3 catalyst are due to the crystallisation of the amorphous Co phase upon an increased partial pressure of water, as seen in Fig. 3e′. There are no correlations, neither overall nor within the same support. Similar "gunshot" plots were also obtained for the other measured o/p ratios (i.e. for C_2, C_4 and C_5) and indicate that readsorption of short α-olefins most probably cannot account for the increase in S_{C5+} upon a reduced space velocity. As higher α-olefins are not appreciably affected by bed residence time [5,8], it may be concluded that differences in α-olefin readsorption in general can only have a minor impact on the change in S_{C5+} upon changes in the space velocity.

The effect, if any, of α-olefin readsorption on S_{C5+} in general, e.g. for different catalysts at similar conversion levels, is discussed in Section 4.2.1.

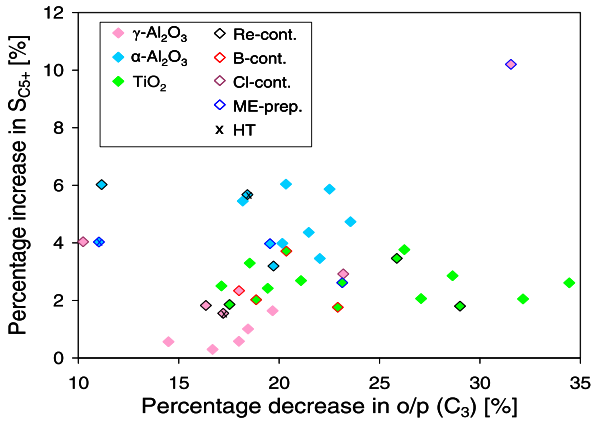

Fig. 6. Percentage increase in S_{C5+} vs. percentage decrease in C_3 olefin/paraffin (o/p) ratio upon halving of the space velocity. Calculations based on selectivity and space velocity data from periods A and B. Experimental conditions as in Fig. 4. ME: microemulsion. HT: hydrothermally treated.

3.3.4. Changing process conditions

3.3.4.1. General observations. Changing the process conditions (e.g. temperature, H_2/CO ratio, catalyst pellet size, addition of water vapour, etc.) changes the α_{Cn} values and selectivities. Fig. 7 shows the resulting changes in α_{C1}–α_{C4} upon some variations in process conditions for three catalysts (Refs 1–3, see caption of Fig. 7). It should be mentioned that the α_{Cn} values for Refs 2 and 3 have been estimated by assuming ASF distribution of the C_{5+} fraction, since C_5 and C_6 data were missing. This gives slightly higher α_{C1} values but does not affect the other α_{Cn} values appreciably. Both the largest absolute changes and the largest deviations from the regression lines obtained under the reference case process conditions lie in the α_{C1}. A higher sensitivity of α_{C1} to changes in partial pressures of H_2 and CO (keeping one of them constant), as well as a lower temperature dependence of α_{C3} and α_{C4} when compared to the other α_{Cn} values, has been reported earlier [21,48]. It has also been reported that the increase in S_{C5+} upon water addition to Co-based catalysts mainly is coupled with a decrease in S_{C1} [29,32], which is in agreement with a relatively large increase in α_{C1}. It should be mentioned that the synthesis gas conversion level was kept constant upon changes in temperature, pellet size [21] and H_2/CO ratio by adjustment of the flow of synthesis gas. In case of water addition, however, no adjustment of synthesis gas flow was made. The conversion level of Ref 1 dropped from 40% to 30% and 20%, by introducing 20% and 33% water vapour, respectively, into the feed gas.

3.3.4.2. Effect of water partial pressure. The effect of external water addition on the α_{Cn} values was investigated in more detail, and the results are illustrated in Fig. 8. New sets of trend lines form for the two different process conditions (20% and 33% water vapour added to the feed, respectively). Part of the overall larger variance in the α_{C1} data upon external water addition, when compared to dry conditions, could be explained by a slightly less accurate temperature control and differences in conversion levels (i.e. partial pressures of water), as each catalyst responds individually with respect to the FT rate upon the addition of water (see Fig. 1) [53]. Furthermore, under the influence of added water vapour, a few data points clearly deviating from the linear relationships are appearing. Those are commented on in Section 3.3.5.

In general, the added water increases the S_{C5+} and, as mentioned above, the largest differences within the studied α_{Cn} values lie in the α_{C1} data, which increase with the amount of added water vapour. The α_{C3} and α_{C4} data points are gathered slightly below their respective regression lines obtained from period B. In Fig. 9, the S_{C1} and S_{C2-C4} vs. S_{C5+} are shown for periods A–D from which it may be seen that a catalyst system having a certain S_{C5+} at dry conditions (period A or B) in general has a significantly higher S_{C1} and somewhat lower S_{C2-C4} compared to a catalyst system that has the same S_{C5+} under the influence of water vapour in the feed. The "reaction pathways" for two selected catalysts going through periods A–D are also illustrated. It should be noted that the addition of water vapour to the feed does not change the slope of the selectivity regression lines.

Fig. 10 shows the change in α_{C1}, α_{C3} and α_{C4} with the average P_{H_2O}/P_{H_2} in the reactor for some selected catalysts (excluding the clearly deviating catalysts discussed in Section 3.3.5). The α_{C1} data points for all these catalysts fall, more or less, into one single curve, while the changes in the higher α_{Cn} values are catalyst specific. It should be mentioned that, in general, no overall effect of Co particle size on the magnitude of the increase in S_{C5+}, either upon a

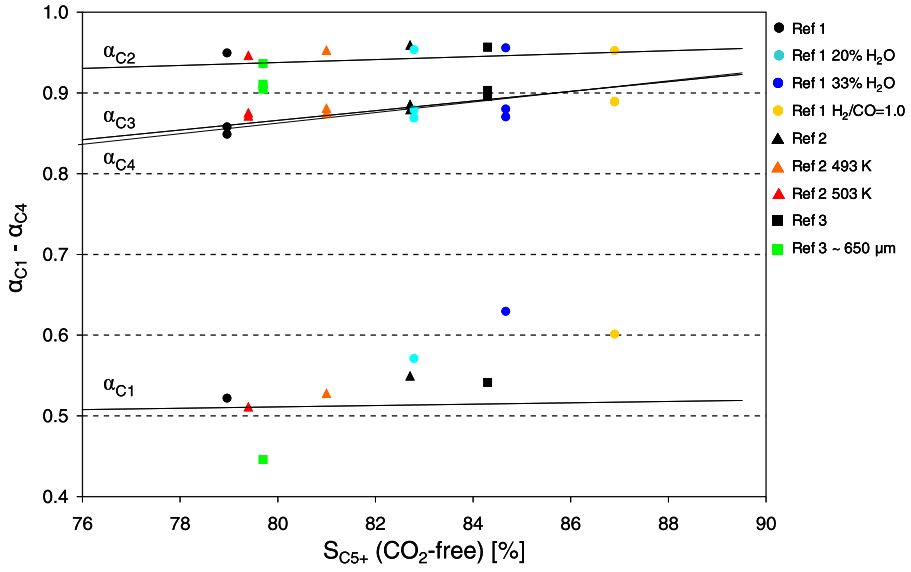

Fig. 7. Effects of changes in process conditions on the α_{Cn} values for three catalysts. The lines are the regression lines from Fig. 4. Reference case conditions: 483 K, 20 bar, inlet H_2/CO = 2.1, pellet size 53–90 µm. ● Ref 1 = 12 wt% Co/γ-Al_2O_3. ▲ Ref 2 = 12 wt% Co/γ-Al_2O_3 (another batch of catalyst). ■ Ref 3 = 20 wt% Co, 0.5 wt% Re/γ-Al_2O_3 (from [21]). The "X% H_2O" indicates that X% of the feed consisted of water vapour.

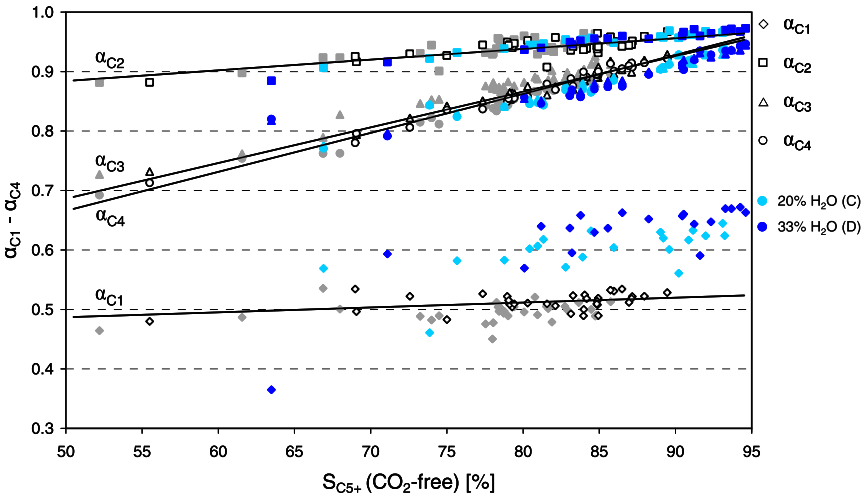

Fig. 8. Effect of external water addition (20% and 33%, respectively) on the α_{Cn} values (n = 1–4) vs. S_{C5+} for all catalysts. Grey, filled symbols indicate period A, open symbols period B and coloured symbols period C and D. Regression lines are based on data points obtained in period B.

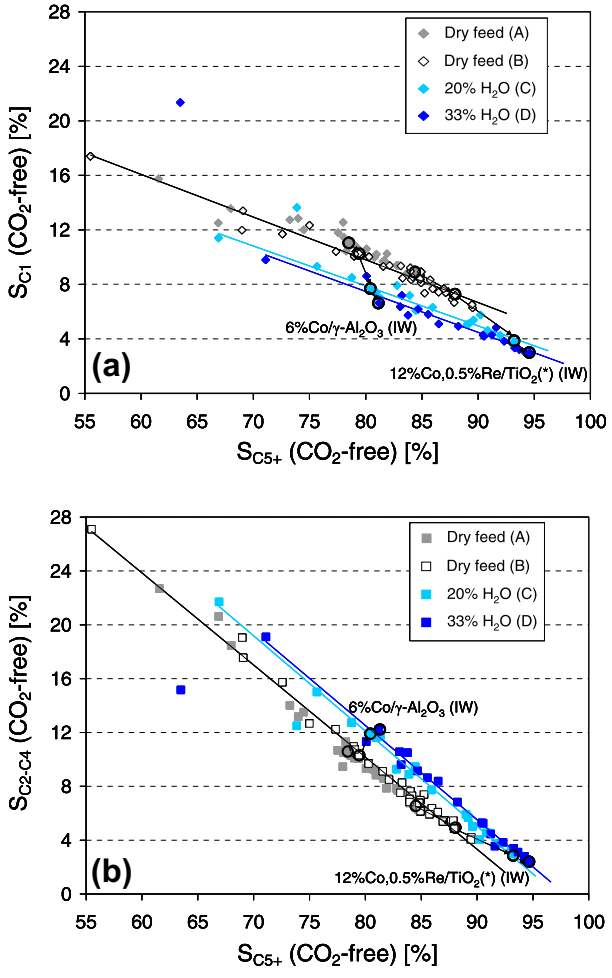

Fig. 9. S_{C1} (a) and S_{C2-C4} (b) vs. S_{C5+} for all catalysts in periods A–D. Regression lines are based on data points obtained in periods B, C and D, respectively, excluding the clearly deviating points in periods C and D. "Reaction pathways" through periods A–D for two catalyst examples are illustrated.

reduction in space velocity (A to B) or upon external addition of water, has been found. However, there is a clear effect of the support material. Typical for the wide-pore-supported catalysts (i.e. TiO_2 and α-Al_2O_3) in this study is a large increase in S_{C5+} upon a lowered space velocity (see Fig. 6) and also a large increase in S_{C5+} upon external water addition. This can be understood from the increasing α_{C1}–α_{C4} values (see Fig. 10) going through periods A–D and is illustrated for 12%Co, 0.5%Re/TiO_2(*) (IW) in Fig. 9. Typical for the narrow-pore-supported catalysts (i.e. γ-Al_2O_3) is a much smaller increase in S_{C5+} with a reduced space velocity and, especially for the catalysts with low Co loadings (i.e. 6 and 8 wt%), the increase in S_{C5+} upon external water addition is very small. Actually, the α_{C2}–α_{C4} values for the 6%Co/γ-Al_2O_3 (IW) catalyst decrease somewhat upon external addition of water vapour (see Fig. 10), which means that although S_{C5+} is slightly increased, so are the S_{C2}, S_{C3} and S_{C4} (see Fig. 9). According to the sparse full product analysis data in the literature, α_{∞} was found to increase when adding water vapour to a Co/Ru/ZrO_2/SiO_2 catalyst [29] and an unsupported Co catalyst [30]. The results in the present study, however, indicate a possibility of water addition to reduce the higher α_{Cn} values, and possibly α_{∞}, although S_{C5+} is increased. This could, for instance, result in a lowered S_{C10+}, which is not desirable if wax is the product aimed for. In fact, the S_{C7+} for the 6%Co/γ-Al_2O_3 (IW) catalyst decreases from 69.5% in period B to 67.7% in period C, while the S_{C5+} increases from 79.4% to 80.4%.

3.3.4.3. Effect of H_2/CO ratio. In Fig. 11a and b, the S_{C1} and S_{C2-C4} vs. S_{C5+} are shown, respectively, for inlet H_2/CO ratios of 2.1 and 1.0. The CO conversion level ranged between 6 and 29% in the experiments with inlet H_2/CO ratios of 1.0, which resulted in reactor-average H_2/CO ratios between 0.8 and 0.97. The lower inlet H_2/CO ratio was only tested for a small proportion of the catalysts, but still there is a clear difference in the selectivity correlations when compared to at the higher inlet H_2/CO ratio. Within the studied S_{C5+} range, a catalyst system having a certain S_{C5+} at inlet H_2/CO = 2.1 in general has a higher S_{C1}, and somewhat lower S_{C2-C4}, compared to a catalyst system that has the same S_{C5+} at inlet H_2/CO = 1.0. As opposed to the effect of water addition to the feed, the change in H_2/CO ratio changes the slopes of the selectivity regression lines. In Fig. 11c, the α_{C1}–α_{C4} values vs. S_{C5+} for inlet H_2/CO = 1.0 are shown, and it is obvious that α_{C1} at these conditions is not invariant with S_{C5+}. It should be mentioned that this observation is not an effect of the small difference in reactor-average H_2/CO ratio.

An example of the effect of lowering the inlet H_2/CO ratio from 2.1 to 1.0 on the selectivity/α_{Cn} values of a single catalyst was given

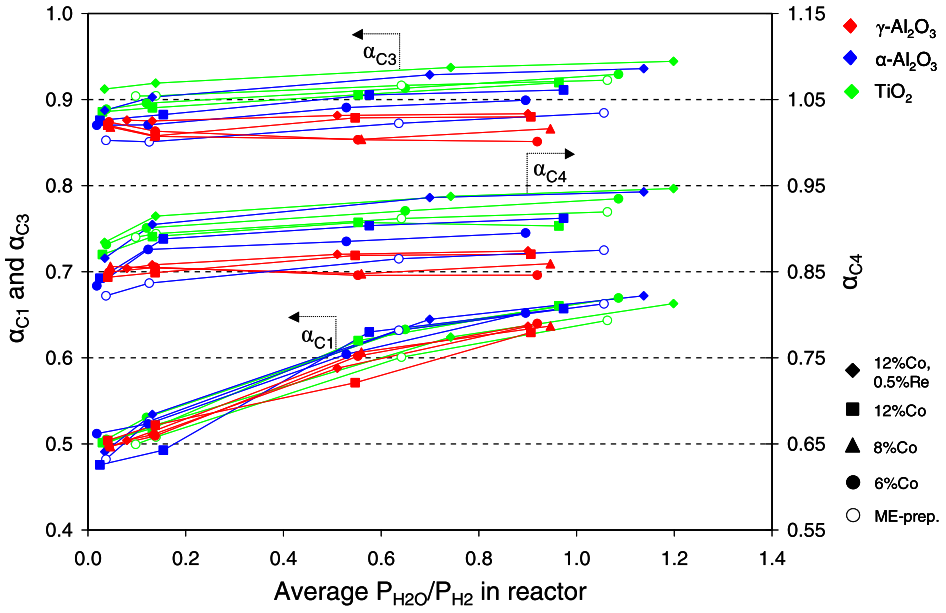

Fig. 10. α_{C1}, α_{C3} and α_{C4} vs. reactor-average P_{H_2O}/P_{H_2} ratio for selected catalysts. The four P_{H_2O}/P_{H_2} ratios for each catalyst are obtained from periods A, B, C and D, respectively.

in Fig. 7 and, obviously, the largest difference lies in the increase of α_{C1} but also an increase in the higher α_{Cn} values may be anticipated, as already reported in the literature [7,48].

3.3.5. Effect of time on stream on selectivity

The majority of the data points from period E, i.e. after five days on stream, still follow the regression lines obtained from period B relatively well. However, for four of the used catalysts, the selectivities/α_{Cn} values deviate significantly from these correlations. The deviating catalysts are the hydrothermally treated 12%Co, 0.5%Re/γ-Al_2O_3 (IW), the one of the two 12%Co, 0.5%Re/α-Al_2O_3 (IW) catalysts with the smallest Co particles (21 compared to 27 nm, or 19 compared to 33 nm if estimated from XRD of calcined catalyst), the ME-γ-Al_2O_3 and the 12%Co, 0.5%Re/γ-Al_2O_3 (IW) prepared from $CoCl_2$ and calcined at 773 K. The two significantly deviating points in period C and D (see Figs. 8 and 9) are for the hydrothermally treated 12%Co, 0.5%Re/γ-Al_2O_3 (IW). Fig. 12 shows the S_{C1} and S_{C2-C4} vs. S_{C5+} in periods B and E, and the deviation of the four catalysts implies that the S_{C1} is increased and the S_{C2-C4} is decreased for a certain S_{C5+}, when compared to the relationships established from period B. Table 3 shows the effect of time on stream on the deviation from the "S_{C1}/S_{C2-C4} vs. S_{C5+}" relationship established from the regression lines in period B (Fig. 5) for all catalysts that were exposed to external water addition. The deviations in period B from this relationship were in the range of ±20% (indicative of the variance in the data from which the relationship is established) while broadening to between −19% and +183% in period E due to the four significantly deviating catalysts. Common characteristics of these catalysts are a relatively large change (positive or negative) in S_{C5+}, comparing at similar conversion levels, going from period A–B to E, as well as a relatively high selectivity to CO_2 in period E (see Table 3), although there are other catalysts showing the same level of S_{CO_2} without significant deviations.

From Table 3, it is evident that the main cause of the deviations is the large decrease in α_{C1} for these four catalysts. The data in Table 3 also show that α_{C1} is in most cases affected by time on stream independently of how the higher α_{Cn} values are affected; for most catalysts, α_{C1} is decreased from A–B to E, while the higher α_{Cn} values have a larger tendency to increase somewhat. This suggests that the mechanism affecting α_{C1} with time on stream is of a different nature than that affecting the higher α_{Cn} values and, presumably, includes the formation of "pure methanation" sites.

The ME-γ-Al_2O_3 catalyst was re-reduced after the 5 days on stream, and it was possible to recover some of the losses in α_{C1} (0.360 → 0.424), which is in agreement with the presence of an oxidised cobalt phase. This phase may possibly be surface CoO, which has been reported to be active for CO_2 formation [54]. The ME-γ-Al_2O_3 catalyst also obtained as high α_{C2}–α_{C4} values as the 12%Co/γ-Al_2O_3 (IW) catalyst, after having crystallised (see Fig. 3e′) and after being re-reduced, which is another indication of that the diffusion distance range in the present study is not an important C-atom selectivity-governing parameter under the prevailing process conditions.

In general, as opposed to the TiO_2 and α-Al_2O_3-supported catalysts, the IW-prepared γ-Al_2O_3 catalysts prepared from $Co(NO_3)_2$ tended to reduce their S_{C5+} somewhat from period A–B to E (see Table 3), however, still following the selectivity regression lines obtained from period B relatively well. This difference lies mainly in the change of the higher α_{Cn} values, and not in the α_{C1} values. Hence, it may be concluded that the Co–Al compounds, reported to form with time on stream for γ-Al_2O_3-supported catalysts [55–60], are not particularly active as "pure methanation" sites.

4. Discussion

4.1. Validity of the estimated α_{Cn} values

By assuming a constant α for $n > 3$, i.e. $\alpha_{C5+} = \alpha_{C4}$, the S_{C5+} was calculated based on the regression lines for α_{C1}–α_{C4} in Fig. 4 and compared with the average measured selectivities (i.e. according to the regression lines in Fig. 5) obtained from the carbon mass balance over the reactor, within the experimental range (i.e. S_{C5+}: 50–90%). The relative error in the calculated S_{C5+} lies within ±1.5%. This satisfactory match between calculated and measured selectivities, however, cannot be used to rule out the existence of two different α values (i.e. α_1 and α_∞) governing the distribution of the higher carbon-number HCs, since the α_{Cn} estimations themselves are built

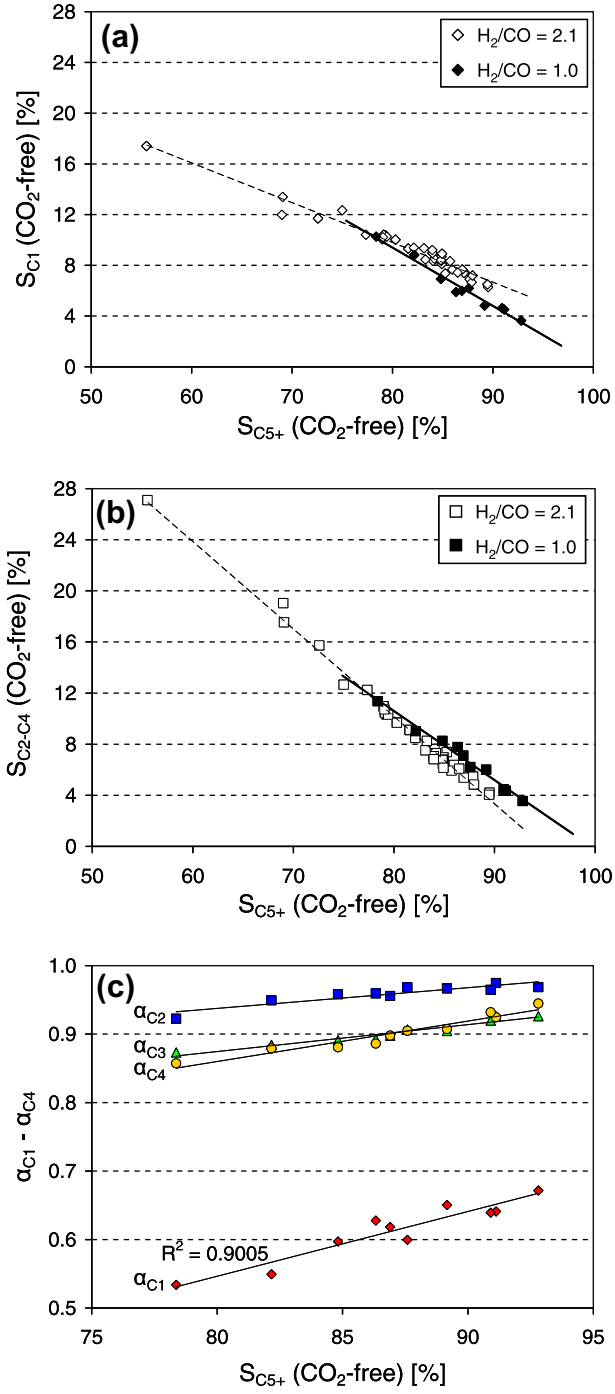

Fig. 11. (a) S_{C1} vs. S_{C5+} for inlet H_2/CO ratios 2.1 (period B) and 1.0. (b) S_{C2-C4} vs. S_{C5+} for inlet H_2/CO ratios 2.1 (period B) and 1.0. (c) α_{Cn} values (n = 1–4) vs. S_{C5+} for inlet H_2/CO = 1.0.

upon the assumption that the C_{7+} fraction has a constant α. The observation that the α_{C4}–α_{C6} values are relatively constant for each catalyst, as mentioned in Section 3.3.2, is, however, not an effect of this assumption. Furthermore, the fact that there are clear relationships between the estimated α_{C1}–α_{C6} values and the S_{C5+} at constant process conditions suggests that if two α values describe the higher carbon-number product distribution, there should reasonably be a catalyst-property-independent correlation between them (for a constant conversion level). The change in α value with carbon number ($\alpha_1 \rightarrow \alpha_\infty$) would then logically be explained by a

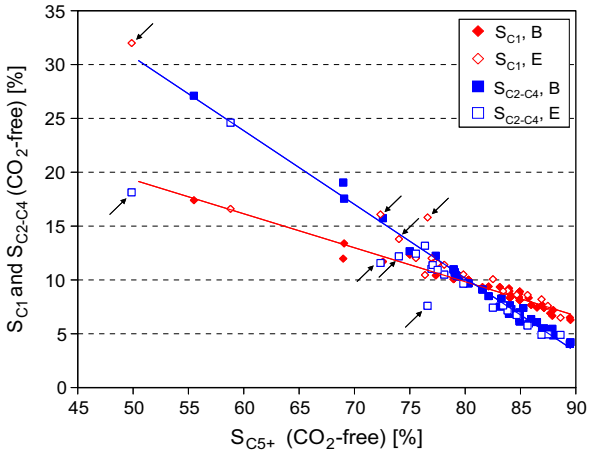

Fig. 12. Illustration of four deviating catalysts: effect of time on stream (including exposure to high partial pressures of water) on the S_{C1} and S_{C2-C4} vs. S_{C5+}, with significantly deviating data points indicated by arrows. The regression lines are based on data points obtained in period B.

chain-length-dependent α-olefin readsorption followed by further chain growth.

It has been reported that α_∞ remains unchanged by changes in space velocity while, for instance, S_{C5+} varies [5]. However, the positions of the "α_{Cn} vs. S_{C5+}" regression lines in Fig. 4 are almost independent of conversion level (space velocity). The estimations of these lower α_{Cn} values (α_{C1}–α_{C4}) are less affected by the C_{7+} assumption and may therefore be considered more accurate and, probably, the correlations between the lower α_{Cn} values and S_{C5+} are indeed more or less independent of conversion level within the studied range.

4.2. Mechanistic considerations

4.2.1. Secondary reactions

In addition to the finding that there are no correlations between changes in S_{C5+} and changes in o/p ratio upon halving of the space velocity (see Fig. 6), there are further observations indicating the minor effect of secondary reactions on S_{C5+} in general. For instance, the relatively high α_{C2} also for the ME-γ-Al_2O_3 catalyst with minor diffusion distance suggests that the low S_{C2} generally observed for Co-based catalysts, as discussed in the introduction, is not due to a high extent of C_2 olefin readsorption but rather due to a particularly high reactivity of the C_2^* surface specie towards chain growth. Alternatively, if the diffusion distances prevailing in the present study are too short to affect the extent of secondary reactions, as it has been shown that α-olefin readsorption takes place also with zero diffusion distance [8], the fact that we obtain different selectivities is in itself a proof of the minor effect of secondary reactions on S_{C5+}.

Borg et al. [20] showed that there was no overall correlation between o/p ratio (for C_3) and S_{C5+} for Co-based catalysts. Correlations only existed within the same support material. The existence of catalyst-property-independent overall correlations between the individual HC selectivities (S_{C1}–S_{C6}) and the S_{C5+}, as shown in the present study, therefore, indicates that different mechanisms govern the production of the sum of the olefin and paraffin and the production of the separate olefin and paraffin (of a specific carbon number), at least for the low carbon numbers investigated in the present study. This, again, suggests that differences in α-olefin readsorption can only have a minor effect on the S_{C5+}, which is in agreement with Kuipers et al. [8] who found that the extent of readsorption with further chain growth of short α-olefins was very small.

Table 3
Effect of time on stream (including exposure to high partial pressures of water) on the deviation from predicted S_{C1}/S_{C2-C4} ratio, and on the α_{Cn} values, for the catalysts exposed to external water addition. Changes in S_{C5+} and S_{C1} from period A–B to E, as well as S_{CO_2} in period E, are also included. The four clearly deviating catalysts in period E are marked with *. IW: incipient wetness impregnation. ME: microemulsion. HT: hydrothermally treated.

Catalyst	Percentage deviation in S_{C1}/S_{C2-C4} ratio from model[a], period B (%)	Percentage deviation in S_{C1}/S_{C2-C4} ratio from model[a], period E (%)	Change in S_{C5+} A–B to E[b] (units of %)	Change in S_{C1} A–B to E[b] (units of %)	S_{CO_2} in period E (%)	Percentage change in α_{Cn} value A–B to E[c] (%)		
						α_{C1}	α_{C3}	α_{C4}
γ-Al_2O_3								
6Co (IW)	+6	+16	−1.9	+0.9	0.8	−1.9	−1.4	−0.7
8Co (IW)	+3	+19	−1.4	+1.0	0.8	−3.3	−0.3	−0.4
12Co (IW)	−1	+20	−0.4	+0.8	0.4	−4.0	0	+0.9
12Co + Re (IW)	+7	+25	−2.1	+1.3	0.6	−4.4	−0.3	−1.6
*12Co + Re (IW) HT	+17	+183	−23.9	+19.4	1.9	−42.9	−7.7	−5.8
*12Co + Re (ME)	+2	+87	+10.6	+0.8	1.1	−16.4	+11	+12.7
12Co + Re (IW) CI 573 K	−1	+2	+3.7	−1.0	1.2	+0.6	+2.5	+3.3
*12Co + Re (IW) CI 773 K	−16	+36	+7.1	+1.0	0.8	−16.0	+6.9	+9.1
α-Al_2O_3								
*12Co + Re (IW)	+20	+140	−5.5	+5.7	1.2	−22.8	+0.4	+1.0
α-Al_2O_3(∗)								
12Co + Re (IW)	−9	+11	+0.7	−0.1	0.5	−0.5	−1.3	+3.1
12Co + Re (IW) HT	+18	+28	+0.3	−0.1	1.0	−0.2	+0.3	+0.3
4.4Co + Re (ME)	−4	+15	−0.9	+0.9	0.3	−3.6	+0.6	0
4.4Co + Re (ME) HT	−6	−8	+1.2	−0.2	0.6	−0.8	+2.6	−0.5
α-Al_2O_3(∗∗)								
6Co (IW)	−7	+14	−0.4	+0.8	1.3	−3.7	+0.2	+2.4
12Co (IW)	+14	+6	+3.4	−1.7	0.9	+6.3	+1.4	+3.0
TiO_2								
12Co + Re (IW)	−3	+5	+1.0	−0.2	0.4	−0.7	+1.1	+1.0
TiO_2(∗)								
6Co (IW)	−7	−19	+2.3	−1.0	0.2	+3.1	+1.9	+1.7
12Co + Re (IW)	−3	+21	−0.2	+0.6	0.5	−4.2	+0.1	+1.5
12Co + Re (ME)	+12	+8	+0.9	−0.8	0.2	+3.9	−0.1	+0.2
TiO_2(∗∗)								
12Co (IW)	+1	+18	+2.6	−0.5	0.5	−2.4	+1.9	+3.3

[a] The model value is the S_{C1}/S_{C2-C4} ratio obtained from the selectivity regression lines in Fig. 5 for the S_{C5+} of the catalyst in period B or E.
[b] The selectivity in period A–B is obtained from inter-/extrapolation of the selectivity values in periods A and B to the same conversion level as in period E.
[c] The α_{Cn} values in period A–B are obtained from inter-/extrapolation of the αC_n values in periods A and B to the same conversion level as in period E.

The suggested correlation between α_1 and α_∞ at constant process conditions (see Section 4.1) implies that, within the range of the studied catalyst variables, possible differences in *pore* residence time – a parameter mostly affecting readsorption of higher α-olefins [5] – do not affect the selectivities (S_{C1}–S_{C5+}) or α_{Cn} values appreciably. This has been confirmed earlier by Rytter et al. [21] who, through a detailed product analysis, found that α_∞ was hardly changed upon an increase in catalyst pellet size from 50 to 650 μm.

4.2.2. Methane production vs. higher HC production

In the following subparagraphs, we present some tentative mechanistic models able to explain our main observations.

4.2.2.1. Possible mechanistic models. The key observations of the present study are as follows:

- linear correlations between selectivity to methane (and other light products) and S_{C5+} and
- a relatively constant α_{C1} for a range of catalysts having widely different S_{C5+} selectivities investigated in a fixed-bed under standard low-temperature FT conditions.

As there are specific correlations between the S_{C1} and the other selectivities under all studied process conditions (see for instance Fig. 5), the methane production rate is intrinsically coupled to the production rate of higher HCs. This is in line with a common pool of precursors (here denoted CH_2^* and referred to as the *monomer*), as suggested previously from SSITKA (steady-state isotopic transient kinetic analysis) measurements [61–63]. The relatively constant site activity of the studied catalysts (see Table 2) indicates further that the rate-determining step is the same irrespective of the length of the HC products and, hence, lies within the formation of the monomer, as proposed earlier by Mims and McCandlish [61] and van Dijk et al. [62,63]. A similar site activity for all the studied catalysts also indicates that the monomer formation takes place at a general Co surface present in all catalysts. In summary, the existence of separate methane-producing sites, as sometimes proposed to explain selectivity variations [6], may be ruled out for the (fresh) studied catalysts. However, as mentioned in Section 3.3.5, four of the catalysts apparently developed such "pure methanation" sites after exposure to high partial pressures of water.

Although there are several proposals for activation steps and intermediate surface species, we denote the key entities simply as CH_2^*, CH_3^* and H*, thus capturing the building blocks of the hydrocarbon chain. Methane formation and chain initiation are, hence, schematically illustrated as follows:

$$CH_3^* + H^* \rightarrow CH_4 \quad (6)$$

$$CH_3^* + CH_2^* \rightarrow C_2H_5^* \quad (7)$$

The chain-growth probability of CH_3^*, α_{C1}, may then be expressed as a function of surface coverages (θ) of the monomer CH_2^* and of H*, and of rate constants (k) to chain growth and termination of CH_3^* as shown below:

$$\alpha_{C1} = \frac{r_{C2+}}{r_{C2+} + r_{C1}} = \frac{k_{g,1} \cdot \theta_{CH_3} \cdot \theta_{CH_2}}{k_{g,1} \cdot \theta_{CH_3} \cdot \theta_{CH_2} + k_{t,1} \cdot \theta_{CH_3} \cdot \theta_H} = \frac{\theta_{CH_2}}{\theta_{CH_2} + \frac{k_{t,1}}{k_{g,1}} \cdot \theta_H} \quad (8)$$

For a constant α_{C1} to occur according to Eq. (8), the surface coverages of CH_2^* and H*, as well as the $k_{t,1}/k_{g,1}$ ratio, need to be the same

for all the catalysts investigated. Relatively constant surface coverages (e.g. θ_H, θ_{CHx}, θ_{CO}, measured by SSITKA) irrespective of Co particle size (>6 nm), support material and HC selectivities have recently been reported in the literature [23,44,45]. The constant $k_{t,1}/k_{g,1}$ ratio could reflect an intrinsic property of an active cobalt surface, i.e. $k_{t,1}$ and $k_{g,1}$ independent of chain-growth probability of the longer chains. This could be rationalised by a two-site model in which methane and (at least) C_2^* are formed at one type of site from the same CH_3^* pool, while further chain growth and termination of the C_{2+} chains (alternatively only termination) take place at a separate subgroup of sites present in low concentration. In this model, the formation of methane and $C_{2(+)}^*$ would take place at the Co surface responsible for the monomer production, i.e. at the general Co surface sites present in all of the studied catalysts and the number of which are estimated from chemisorption measurements. The α_{C2+} values and, hence, the S_{C5+} would depend on the ratio of the number and/or activity of the two types of sites.

An alternative explanation to the relatively constant $k_{t,1}/k_{g,1}$ ratio is that it is a coincidence for the chosen process conditions and that both $k_{t,1}$ and $k_{g,1}$ vary (in the same direction) with the S_{C5+} of the catalysts. Again, a two-site model is envisioned in which the monomer and methane are the only products from the general Co surface sites. The monomers not converted into methane then migrate to separate chain-growth sites (also capable of termination) present in low concentration, to form all possible products (including methane). Similar two-site models with migrating monomers have been proposed earlier [63,64]. An apparent constant overall α_{C1} at certain process conditions could be the result of the "extra" production of methane taking place at the general Co sites, whereas the α_{Cn} values at the chain-growth sites are all increasing with the S_{C5+} and governed by the ratio of the number and/or activity of the two types of sites. Supporting evidence for two routes responsible for methane production over Co-based FT catalysts can also be found in the literature [23,45,62,63,65].

4.2.2.2. Further remarks on selectivity. The results from the experiments with an inlet H_2/CO ratio of 1.0 indicate that α_{C1} is not invariant with S_{C5+} for all process conditions. This is possible to explain with the model in which methane production takes place at two types of sites. With an inlet H_2/CO ratio of 2.1 (periods A and B), the lowest theoretical S_{C1} approaches 5% (at S_{C5+} = 95%), extrapolating the regression lines of Fig. 9 to S_{C2-C4} = 0% (i.e. α_{C2+} = 1). Similarly, we can estimate the lowest S_{C1} upon addition of 20% and 33% water to the feed at 3% and 2%, respectively. Apparently, water inhibits the "extra" methane production at the general Co surface, which is further indicated by the similar change in α_{C1} with changes in the average P_{H_2O}/P_{H_2} for the studied catalysts. The general and unequivocal effect of water on the selectivity observed for all catalysts, hence, seems to be limited to this general Co surface.

When the inlet H_2/CO ratio is lowered to 1.0, there seems to be no "extra" production of methane, as both S_{C1} and S_{C2-C4} approaches zero approximately at S_{C5+} = 100% (see Fig. 11a and b), which could explain why α_{C1} now is increasing with S_{C5+} (see Fig. 11c). However, the effect of the H_2/CO ratio is believed to be related to both types of sites by means of changing the relative abundance of the monomer and of hydrogen on the total cobalt surface and thereby directly affecting, for instance, the termination rate at the subgroup sites. The difference in selectivity correlations when adding water and when reducing the inlet H_2/CO ratio, as seen from Figs. 9 and 11, suggests that the positive effect of water on S_{C5+} is not directly linked to a lower surface coverage of hydrogen.

In addition to different extents of secondary reactions caused by differences in mass transfer limitations [2], local differences in availability of adsorbed hydrogen (e.g. due to differences in spillover capacity of the support materials or due to TiO_x decoration) [25,28] or monomeric carbon [24] have been proposed to explain the differences in S_{C5+} among various Co-based catalysts (with Co particles >6 nm). Irrespective of the above proposed mechanistic models, the observation that the overall α_{C1} is more or less the same for all catalysts at the reference case process conditions, and with external water addition, indicates that the differences in S_{C5+} between the catalysts in the present study, however, cannot be ascribed to differences in surface coverages at the general Co surface. However, varying availability of hydrogen and monomeric carbon at the Co/support interfacial perimeter (i.e. at non-general Co sites) cannot be excluded.

Finally, it should be commented that the interrelationships observed in the present study probably do not apply generally for catalysts with Co particles smaller than approximately 6 nm, as it was recently shown that such particles differ considerably in their surface coverages (e.g. θ_H, θ_{CHx}, θ_{CO}) compared to larger Co particles [23].

5. Conclusions

In the range of the studied process conditions and catalyst variables, there is a specific interrelationship (for fixed process conditions) between the HC selectivities also for the non-ASF distributed part of the FT product spectrum (i.e. $\sim C_1$–C_5) irrespective of the properties of the Co-based catalyst. Hence, there is a mechanistic link between the formation of methane and higher HCs, presumably a common precursor (monomer) pool, and the existence of "pure methanation" sites may, therefore, be ruled out for the (fresh) studied catalysts. It is noteworthy that α_{C1} is more or less constant for 36 catalysts exposing a large S_{C5+} range, when investigated at standard low-temperature FT conditions (H_2/CO = 2.1). This indicates that although resulting from a common pool of intermediates, the mechanism of methane formation differs from that of higher HCs. It seems, however, like the constant α_{C1} behaviour is not valid at other H_2/CO ratios.

For a small proportion of the studied catalysts, the exposure to high partial pressures of water seemingly involved changes in the surface composition, may be to CoO, resulting in the formation of "pure methanation" sites possibly responsible for a separate precursor pool. Surface Co–Al compounds reported to form in Co/γ-Al_2O_3 catalysts with time on stream were, however, found not to be particularly active as "pure methanation" sites.

For the conditions studied, the reason for a high S_{C5+} is found to be essentially a high intrinsic chain-growth probability and not a result of an enhanced α-olefin readsorption. The increase in S_{C5+} upon a reduction in space velocity is, therefore, at least partially believed to be due to the higher partial pressure of water as a result of an increased conversion level. The linear interdependencies between the propagation probabilities α_{Cn} as a function of S_{C5+} vary with process conditions; however, α_{C1} is in most cases significantly more affected than the other α_{Cn} values. A lowered space velocity, as well as external water addition, increases the S_{C5+} for essentially all catalysts. However, the individual response in α_{C2}–α_{C4} values and selectivities upon water exposure varies greatly with catalyst and, seemingly, mostly with the choice of support material, while α_{C1} is affected in a similar way for all catalysts (except for the catalysts developing "pure methanation" sites). The general and unequivocal effect of water addition on the hydrocarbon selectivities is found to be limited to the decrease in S_{C1}. Reducing the H_2/CO ratio also increases the S_{C5+} but results in different selectivity interdependencies compared to when increasing the water partial pressure.

In the present study, careful quantitative analysis was only made of the C_1–C_4 HC products. The data, therefore, do not provide evidence for a catalyst-property-independent correlation between

the lower HC selectivities and α_{∞} (at constant process conditions and conversion levels), although there are such indications.

Acknowledgments

The authors acknowledge the financial support provided by the Swedish Energy Agency. Odd Asbjørn Lindvåg and Rune Myrstad, SINTEF Materials and Chemistry, Trondheim, are gratefully acknowledged for help during the experimental part of the work. We also thank Li He, Department of Chemical Engineering, NTNU, Trondheim, for performing the HYSYS calculations. Professor De Chen and Paul Radstake, Department of Chemical Engineering, NTNU, Trondheim, and Robert Andersson, Chemical Technology, KTH, Stockholm, are gratefully acknowledged for fruitful discussions.

References

[1] E. Iglesia, S.C. Reyes, R.J. Madon, J. Catal. 129 (1991) 238.
[2] E. Iglesia, S.L. Soled, R.A. Fiato, J. Catal. 137 (1992) 212.
[3] G.P. van der Laan, A.A.C.M. Beenackers, Catal. Rev. – Sci. Eng. 41 (1999) 255.
[4] T. Riedel, H. Schulz, G. Schaub, K. Jun, J. Hwang, K. Lee, Top. Catal. 26 (2003) 41.
[5] R.J. Madon, E. Iglesia, S.C. Reyes, in: S.L. Suib, M.E. Davis (Eds.), Selectivity in Catalysis, American Chemical Society, Washington, DC, 1993, p. 382.
[6] H. Schulz, Stud. Surf. Sci. Catal. 163 (2007) 177.
[7] C.G. Visconti, E. Tronconi, L. Lietti, R. Zennaro, P. Forzatti, Chem. Eng. Sci. 62 (2007) 5338.
[8] E.W. Kuipers, C. Scheper, J.H. Wilson, I.H. Vinkenburg, H. Oosterbeek, J. Catal. 158 (1996) 288.
[9] J. Patzlaff, Y. Liu, C. Graffmann, J. Gaube, Appl. Catal. A 186 (1999) 109.
[10] J. Patzlaff, Y. Liu, C. Graffmann, J. Gaube, Catal. Today 71 (2002) 381.
[11] J. Gaube, H.F. Klein, J. Mol. Catal. A: Chem. 283 (2008) 60.
[12] R.A. Dictor, A.T. Bell, J. Catal. 97 (1986) 121.
[13] B.W. Wojchiechowski, Catal. Rev. – Sci. Eng. 30 (1988) 629.
[14] I. Puskas, R.S. Hurlbut, R.E. Pauls, J. Catal. 139 (1993) 591.
[15] M. Inoue, T. Miyake, T. Inui, J. Catal. 105 (1987) 266.
[16] P.A. Jacobs, D. van Wouwe, J. Mol. Catal. 17 (1982) 145.
[17] V. Ponec, Catal. Rev. – Sci. Eng. 18 (1978) 151.
[18] H. Schulz, E. van Steen, M. Claeys, Stud. Surf. Sci. Catal. 81 (1994) 455.
[19] Ø. Borg, S. Eri, E.A. Blekkan, S. Storsæter, H. Wigum, E. Rytter, A. Holmen, J. Catal. 248 (2007) 89.
[20] Ø. Borg, P.D.C. Dietzel, A.I. Spjelkavik, E.Z. Tveten, J.C. Walmsley, S. Diplas, S. Eri, A. Holmen, E. Rytter, J. Catal. 259 (2008) 161.
[21] E. Rytter, S. Eri, T.H. Skagseth, D. Schanke, E. Bergene, R. Myrstad, A. Lindvåg, Ind. Eng. Chem. Res. 46 (2007) 9032.
[22] G.L. Bezemer, J.H. Bitter, H.P.C.E. Kuipers, H. Oosterbeek, J.E. Holewijn, X. Xu, F. Kapteijn, A.J. van Dillen, K.P. de Jong, J. Am. Chem. Soc. 128 (2006) 3956.
[23] J.P. den Breejen, P.B. Radstake, G.L. Bezemer, J.H. Bitter, V. Frøseth, A. Holmen, K.P. de Jong, J. Am. Chem. Soc. 131 (2009) 7197.
[24] C.A. Mims, C.J. Bertole, Stud. Surf. Sci. Catal. 136 (2001) 375.
[25] D. Schanke, S. Eri, E. Rytter, C. Aaserud, A.M. Hilmen, O.A. Lindvåg, E. Bergene, A. Holmen, Stud. Surf. Sci. Catal. 147 (2004) 301.
[26] S. Storsæter, Ø. Borg, E.A. Blekkan, B. Tøtdal, A. Holmen, Catal. Today 100 (2005) 343.
[27] S. Krishnamoorthy, M. Tu, M.P. Ojeda, D. Pinna, E. Iglesia, J. Catal. 211 (2002) 422.
[28] E. Iglesia, Appl. Catal. A 161 (1997) 59.
[29] H. Schulz, M. Claeys, S. Harms, Stud. Surf. Sci. Catal. 107 (1997) 193.
[30] C.J. Bertole, C.A. Mims, G. Kiss, J. Catal. 210 (2002) 84.
[31] D. Tristantini, S. Lögdberg, B. Gevert, Ø. Borg, A. Holmen, Fuel Process. Technol. 88 (2007) 643.
[32] S. Storsæter, Ø. Borg, E.A. Blekkan, A. Holmen, J. Catal. 231 (2005) 405.
[33] Ø. Borg, M. Rønning, S. Storsæter, W. van Beek, A. Holmen, Stud. Surf. Sci. Catal. 163 (2007) 255.
[34] C.H. Bartholomew, Catal. Lett. 7 (1990) 27.
[35] J.L. Lemaitre, P. Govind Menon, F. Delannay, in: F. Delannay (Ed.), Characterization of Heterogeneous Catalysts, vol. 15, Marcel Dekker, Inc., New York, 1984, pp. 299–365.
[36] R.C. Reuel, C.H. Bartholomew, J. Catal. 85 (1984) 63.
[37] R.D. Jones, C.H. Bartholomew, Appl. Catal. 39 (1988) 77.
[38] D. Schanke, S. Vada, E.A. Blekkan, A.M. Hilmen, A. Hoff, A. Holmen, J. Catal. 156 (1995) 85.
[39] A.Y. Khodakov, R. Bechara, A. Griboval-Constant, Appl. Catal. A 254 (2003) 273.
[40] A. Moen, D.G. Nicholson, M. Rønning, H. Emerich, J. Mater. Chem. 8 (1998) 2533.
[41] A.M. Hilmen, D. Schanke, A. Holmen, Catal. Lett. 38 (1996) 143.
[42] J. Li, N.J. Coville, Appl. Catal. A 181 (1999) 201.
[43] S. Storsæter, B. Tøtdal, J.C. Walmsley, B.S. Tanem, A. Holmen, J. Catal. 236 (2005) 139.
[44] V. Frøseth, S. Storsæter, Ø. Borg, E.A. Blekkan, M. Rønning, A. Holmen, Appl. Catal. A 289 (2005) 10.
[45] V. Frøseth, Ph.D. Thesis, Norwegian University of Science and Technology (NTNU), 2006
[46] P.J. Flory, J. Am. Chem. Soc. 58 (1936) 1877.
[47] R.A. Friedel, R.B. Anderson, J. Am. Chem. Soc. 72 (1950) 1212–2307.
[48] C.J. Bertole, G. Kiss, C.A. Mims, J. Catal. 223 (2004) 309.
[49] S. Hinchiranan, Y. Zhang, S. Nagamori, T. Vitidsant, N. Tsubaki, Fuel Process. Technol. 89 (2008) 455.
[50] T. Komaya, A.T. Bell, Z. Weng-Sich, R. Gronsky, F. Engelke, T.S. king, M. Pruski, J. Catal. 150 (1994) 400.
[51] J.L. Li, N.J. Coville, S. Afr. J. Chem. 56 (2003) 1.
[52] E. Iglesia, S.C. Reyes, R.J. Madon, S.L. Soled, Adv. Catal. 39 (1993) 221.
[53] Ø. Borg, S. Storsæter, S. Eri, H. Wigum, E. Rytter, A. Holmen, Catal. Lett. 107 (2006) 95.
[54] D.S. Newsome, Catal. Rev. – Sci. Eng. 21 (1980) 27.
[55] A. Tavasoli, R.M.M. Abbaslou, A.K. Dalai, Appl. Catal. A 346 (2008) 58.
[56] G. Jacobs, P.M. Patterson, T.K. Das, M. Luo, B.H. Davis, Appl. Catal. A 270 (2004) 65.
[57] G. Jacobs, Y. Zhang, T.K. Das, J. Li, P.M. Patterson, B.H. Davis, Stud. Surf. Sci. Catal. 139 (2001) 415.
[58] D. Schanke, A.M. Hilmen, E. Bergene, K. Kinnari, E. Rytter, E. Ådnanes, A. Holmen, Catal. Lett. 34 (1995) 269.
[59] D. Schanke, A.M. Hilmen, E. Bergene, K. Kinnari, E. Rytter, E. Ådnanes, A. Holmen, Energy Fuels 10 (1996) 867.
[60] A.M. Hilmen, D. Schanke, K.F. Hanssen, A. Holmen, Appl. Catal. A 186 (1999) 169.
[61] C.A. Mims, L.E. McCandlish, J. Phys. Chem. 91 (1987) 929.
[62] H.A.J. Van Dijk, J.H.B.J. Hoebink, J.C. Schouten, Stud. Surf. Sci. Catal. 130 (2000) 383.
[63] H.A.J. Van Dijk, J.H.B.J. Hoebink, J.C. Schouten, Top. Catal. 26 (2003) 111.
[64] H. Schulz, Z. Nie, F. Ousmanov, Catal. Today 71 (2002) 351.
[65] S. Vada, B. Chen, J.G. Goodwin Jr., J. Catal. 153 (1995) 224.